Problèmes inverses en électrocardiographie et en tomographie par impédance électrique

Lisl Weynans

Bordeaux University, INRIA and IHU Liryc

Canum 2026

Context

Electrical activity of the heart

- electrical activation : propagation of an activation front, initiating cardiac contraction
- dysfonctioning in electrical activity leads to cardiac arythmias

IHU Liryc : Institute of Heart Rythm Diseases

- combines clinical, experimental and numerical research in the area of cardiac arrhythmias

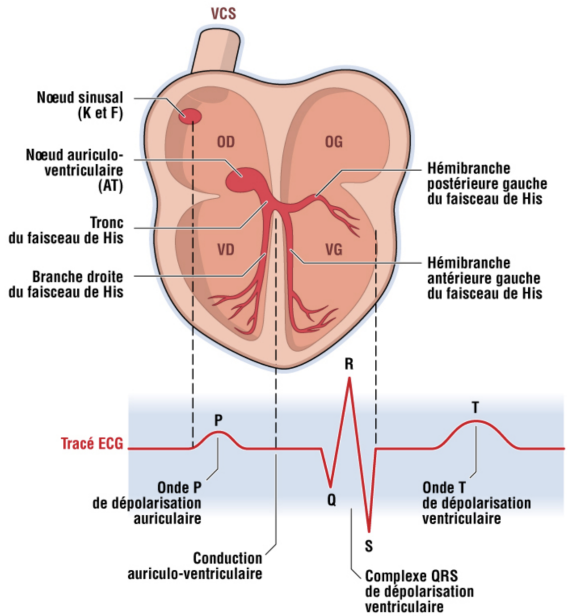

Propagation of activation front

Cardiac action potential :

- 0 : depolarization, activation of cardiac cell
- 2 : plateau zone, activated cell

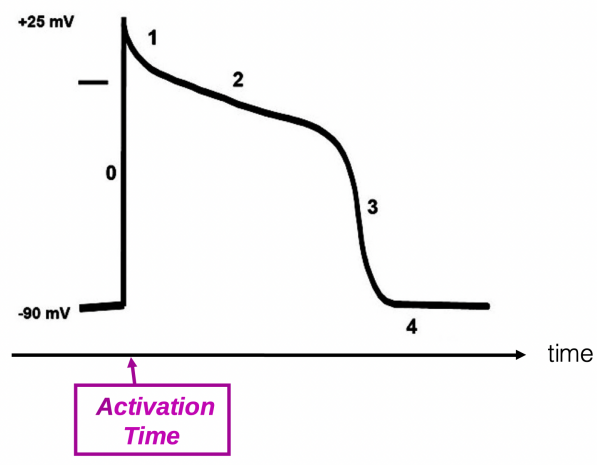

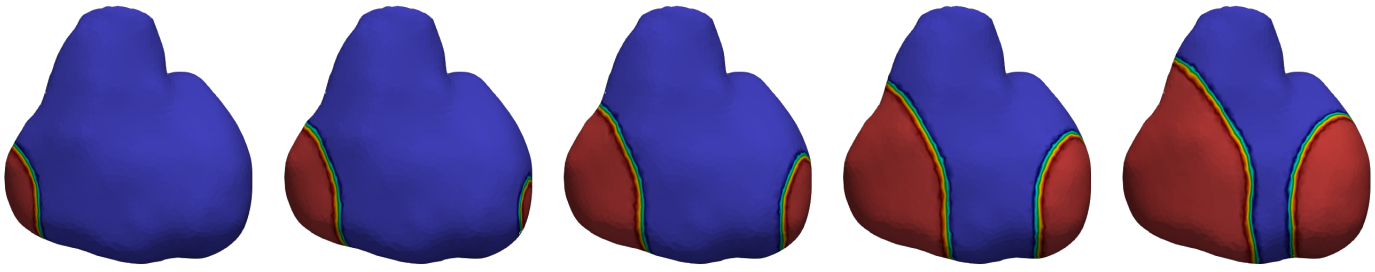

Ventricular fibrillation

- Sudden cardiac deaths : 10 % of deaths worldwide
- among them : 70 % due to ventricular fibrillation (VF) : asynchrone and very fast pulsations, ventricules cannot contract, leads to death within minutes if no intervention
- very low survival rate ($\approx 4\%$), while cardiopulmonary resuscitation and rapid defibrillation can restore normal heart rhythm

Fundamental issue : identifying people at risk

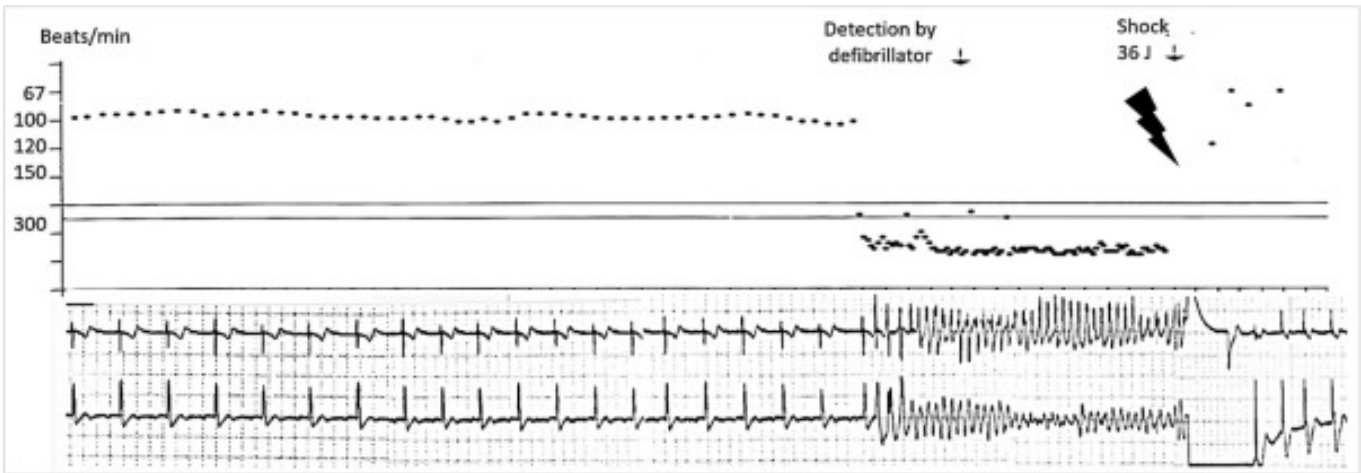

Haissaguerre et al. 2024 : Patient resuscitated from VF at age of 22. He had a single recurrence 19 years later. The recurrence trace shows the absence of prior events and the sudden nature of VF. The defibrillator detects the arrhythmia and delivers a shock to restore normal rhythm.

Electrocardiographic Inverse Problem : ECGi

- Non-invasive imaging modality to reconstruct electrical cardiac activation
- Widely studied since 40 years : Rudy 80, Colli-Franzone 85, Ben Abda et al 11, Cluitmans et al 15, Karoui et al 18, Amri et al 22...

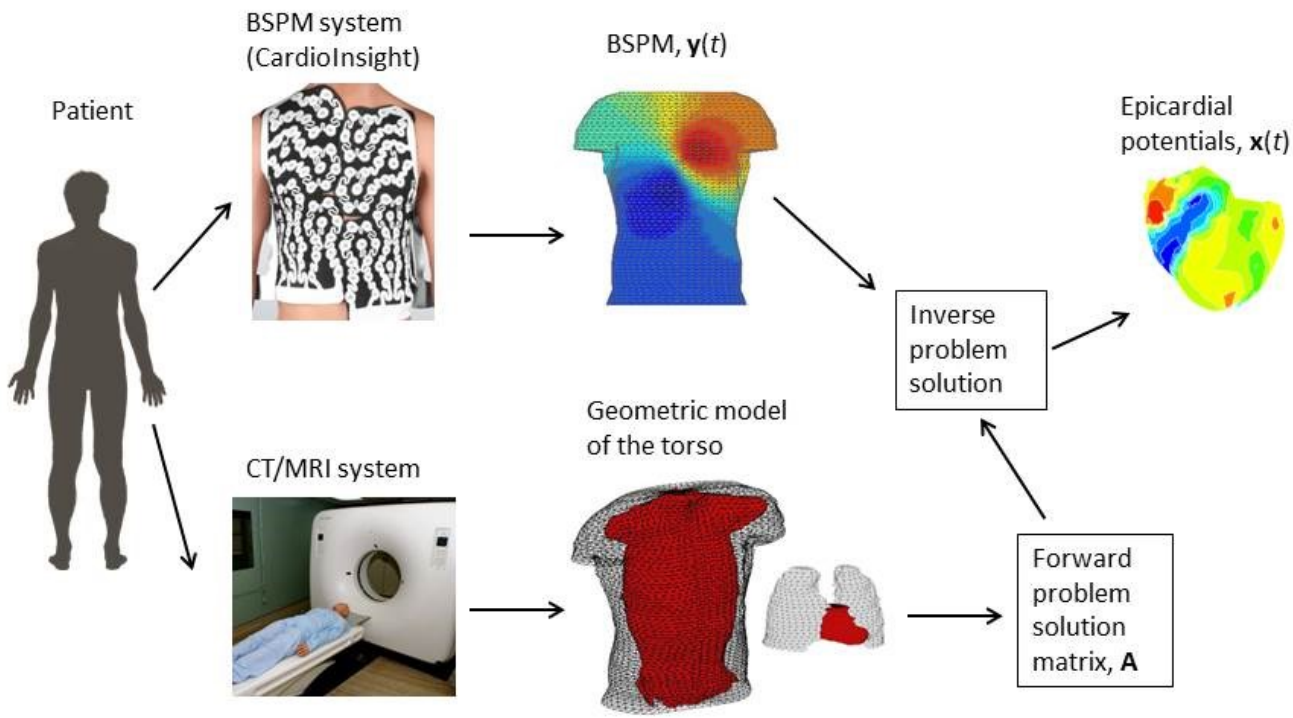

Classical Electrocardiographic Inverse Problem

Cauchy problem for Laplace equation

$$
\begin{aligned}
-\operatorname{div}(\sigma_T \nabla u) &= 0 && \text{dans } \Omega_T \\
u &= z_T && \text{sur } \Gamma_T \\
\sigma_T \partial_n u &= 0 && \text{sur } \Gamma_T
\end{aligned}
$$

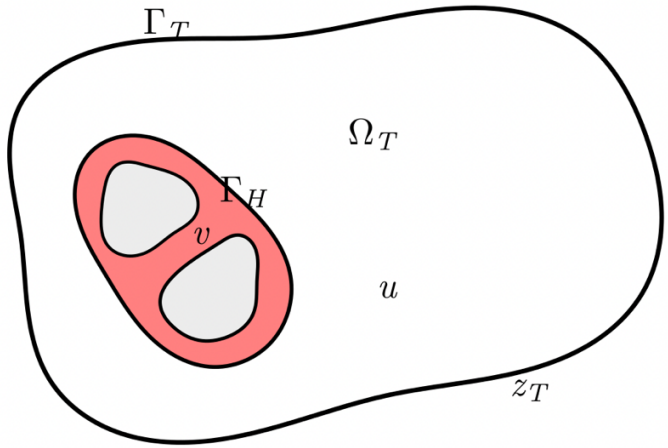

$$\operatorname{argmin}\left(||Ax - z_T||^2 + \epsilon R(x)\right)$$

- z_T measured potentials on surface torso
- x electric source (heart surface)
- A direct operator
- $R(x)$ regularization term

Activation maps : visualization of

- block lines
- starting points of activation

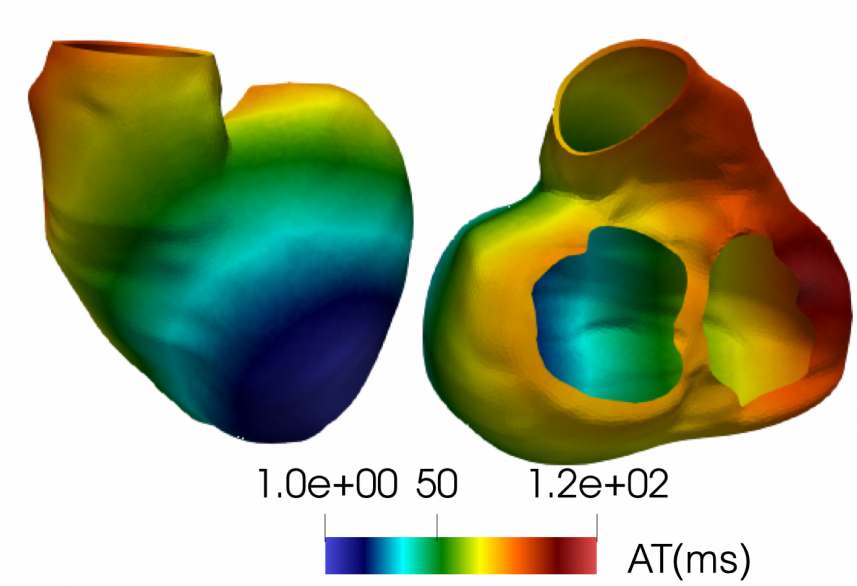

Electrocardiographic Inverse Problem

Current performances of ECGi :

- In-silico studies : OK (even if not accurate)
- Ex-vivo studies : in the torso tank experimental set up developed at Liryc : OK if no error on electrodes location
- In-vivo studies : ok only for regular electrical activation patterns

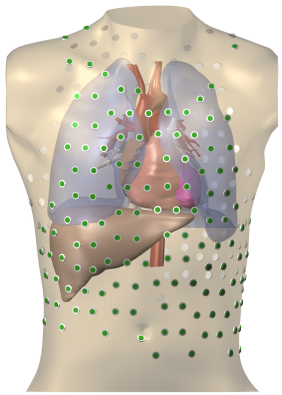

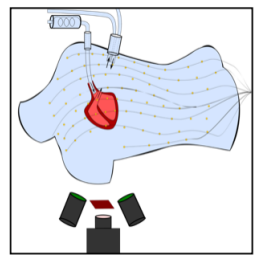

Electrocardiographic Inverse Problem

Error sources/possible improvements

- experimental noise
- inverse problem resolution (local minima, numerical artifacts..)
- modelling of direct problem, accounting for realistic, heterogeneous, moving, torso volume

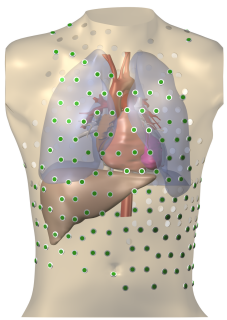

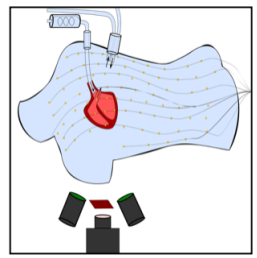

Electrocardiographic Inverse Problem

1. A new epicardial model for ECGi
2. An immersed boundary method for Electrical Impedance Tomography

Modelling of cardiac electrical activity

Joint work : : Emma Lagracie, Yves Coudière

Bidomain model coupled with torso

Anisotropic diffusion

Reaction: ionic model, coupled with EDOs

$$
\begin{aligned}
&\operatorname{div}(\sigma_i \nabla(u+v)) = \partial_t v + I_{ion}(v,t,h) && \Omega_H \times [0,T] \\
&\operatorname{div}((\sigma_e+\sigma_i)\nabla u) = -\operatorname{div}(\sigma_i \nabla v) && \Omega_H \times [0,T] \\
&\operatorname{div}(\sigma_T \nabla u) = 0 && \Omega_T \times [0,T] \\
&\sigma_i \nabla(u+v)\cdot n = 0 && \partial\Omega_H \times [0,T] \\
&\sigma_T \nabla u \cdot n = 0 && \partial\Omega_T \times [0,T]
\end{aligned}
$$

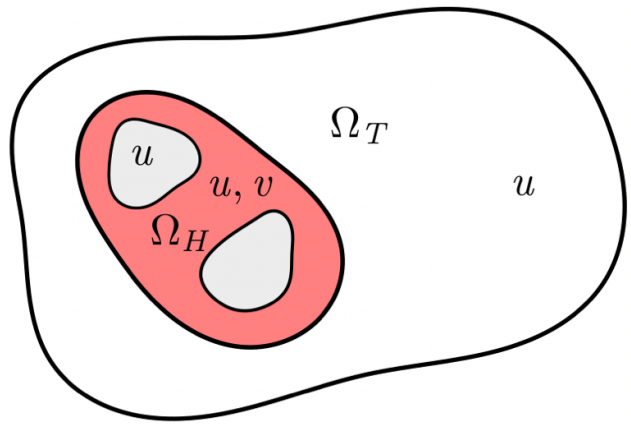

Diffusion: Laplace equation in the torso

A new epicardial model

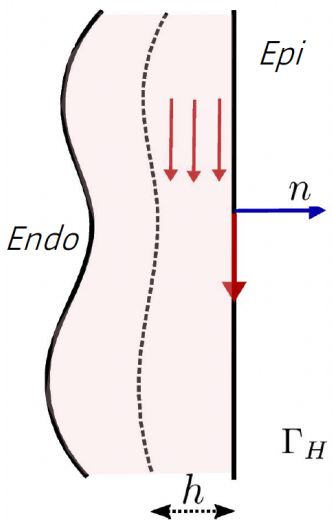

Ω_T

Γ_T

à calibrer

$$\begin{aligned} &\mathrm{div}_S(h(x)(\sigma_i^S + \sigma_e^S)\nabla_S \bar{u})) + \sigma_T \nabla u \cdot n \\ &= -\mathrm{div}_S(h(x)(\sigma_i^S \nabla_S v)) && \Gamma_H \\ &\mathrm{div}(\sigma_T \nabla u) = 0 && \Omega_T \end{aligned}$$

$$\begin{aligned} &\sigma_T \nabla u \cdot n = 0 && \Gamma_T \\ &\sigma^n \frac{u - \bar{u}}{\alpha h} = \sigma_T \nabla u \cdot n && \Gamma_H \end{aligned}$$

- more modelling options : conductivities, activation status of v....
- naturally substituting to the classical Cauchy problem

ECGi with new epicardial model

Epicardial model + Tikhonov

$$\min J(u,v) = \frac{1}{2}\int_{\Gamma_T} |u - z_T|^2 + \frac{\varepsilon}{2}\int_{\Gamma_H} |\nabla v|^2 + \frac{\varepsilon_{\text{inv}}}{2}\int_{\Gamma_H} |v|^2$$

Classical Cauchy + Tikhonov

$$\min J_{pp}(u) = \frac{1}{2}\int_{\Gamma_T} |u - z_T|^2 + \frac{\varepsilon}{2}\|\nabla u\|^2_{L^2(\Gamma_H)}$$

+ EDP constraints :

$$\begin{aligned}
&\text{div}_S(h(x)(\sigma_i^S + \sigma_e^S)\nabla_S \bar{u})) + \sigma_T \nabla u \cdot n \\
&= -\text{div}_S(h(x)(\sigma_i^S \nabla_S v)) && \Gamma_H \\
&\text{div}(\sigma_T \nabla u) = 0 && \Omega_T
\end{aligned}$$

$$\begin{aligned}
&-\text{div}(\sigma_T \nabla u) = 0 && \Omega_T \\
&u = u_H && \Gamma_H \\
&\sigma_T \partial_n u = 0 && \Gamma_T
\end{aligned}$$

ECGi with new model : activation maps

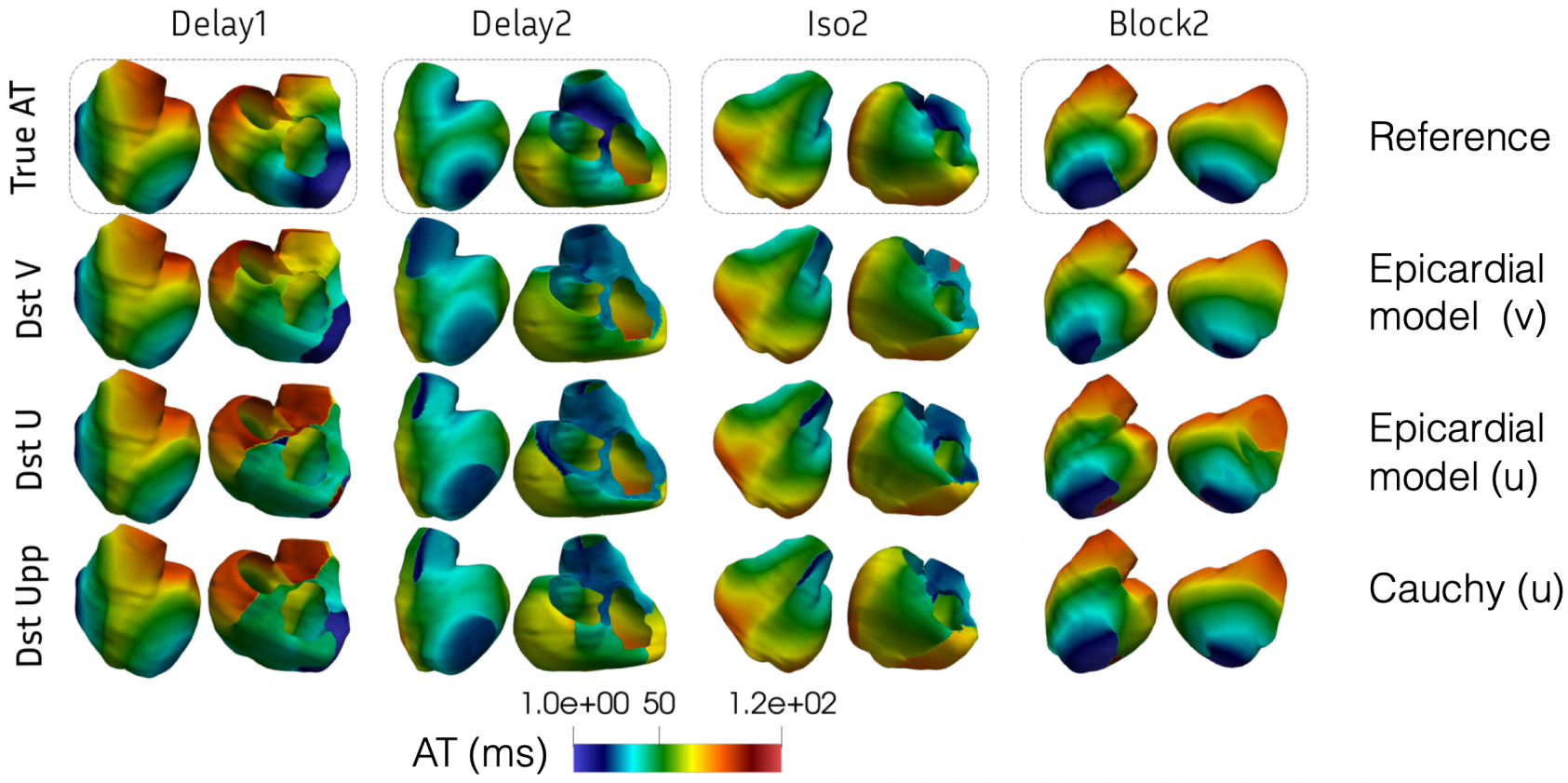

Validation : results similar to classical Cauchy problem, in spite of the approximations made

ECGi with new model : TV regularization

Epicardial model + TV on v + L1 on data

$$\arg\min J_{L1TV}((\bar{u},u),v) = \int_{\Gamma_T} |u - z_T| + \varepsilon \int_{\Gamma_H} |\nabla v| + \frac{\varepsilon_{inv}}{2} \int_{\Gamma_H} |v|^2$$

+ EDP constraint:

$$\begin{aligned} &\mathrm{div}_S(h(x)(\sigma_i^S + \sigma_e^S)\nabla_S \bar{u})) + \sigma_T \nabla u \cdot n \\ &= -\mathrm{div}_S(h(x)(\sigma_i^S \nabla_S v)) && \Gamma_H \\ &\mathrm{div}(\sigma_T \nabla u) = 0 && \Omega_T \end{aligned}$$

Introduction of non-linearities and non-differentiable terms

ECGi with new model : TV regularization

$$\int_{\Gamma_H} |u| \approx \int_{\Gamma_H} \frac{u^2}{\sqrt{u^2+\beta}} \approx \int_{\Gamma_H} \frac{u^2}{\sqrt{\tilde{u}^2+\beta}}$$

$$((\bar{u}^{k+1}, u^{k+1}), v^{(k+1)}) := \underset{((\bar{u},u),v)\in\mathcal{E}}{\arg\min} \frac{1}{2} \int_{\Gamma_T} \frac{(u - z_T)^2}{\sqrt{(u^k - z_T)^2 + \beta}} + \frac{\varepsilon}{2} \int_{\Gamma_H} \frac{\nabla v \cdot \nabla v}{\sqrt{||\nabla v^k||_2^2 + \beta}} + \frac{\varepsilon_{\text{inv}}}{2} \int_{\Gamma_H} v^2$$

Quadratic again !

TV regularization : potentials

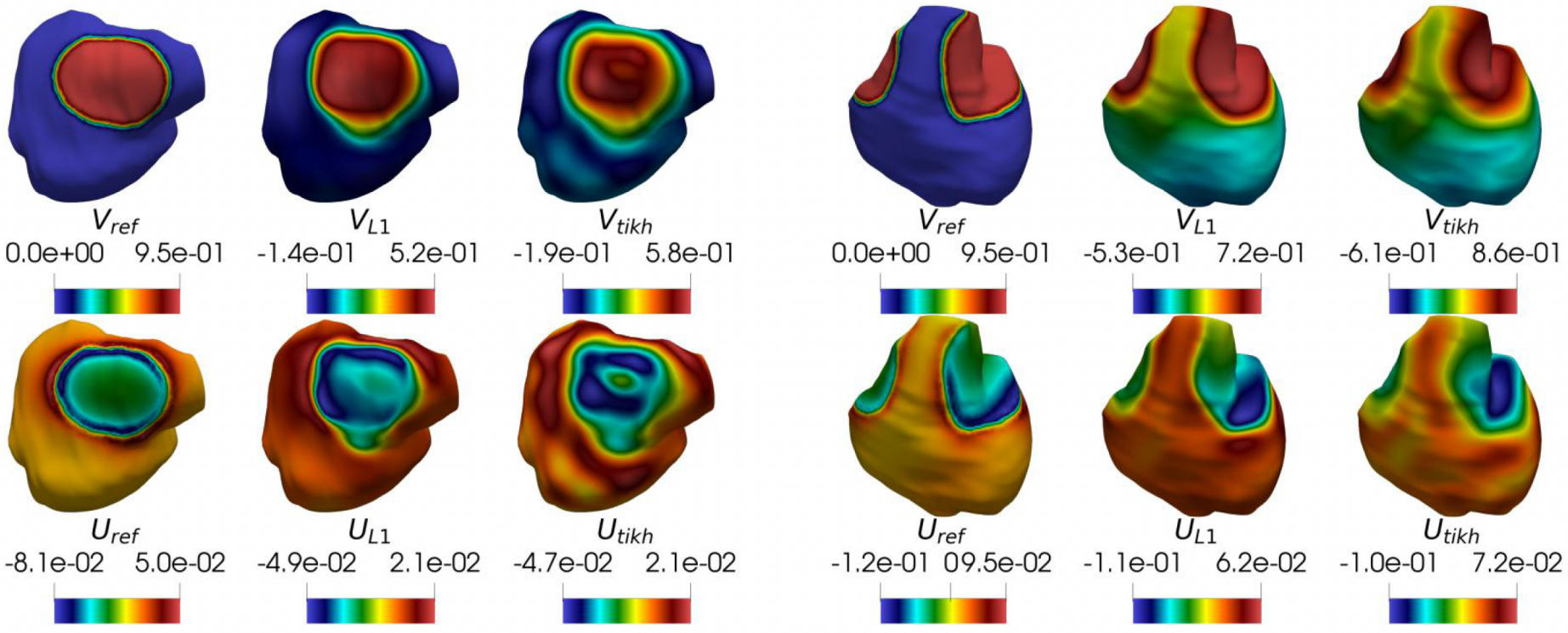

TV regularization : activation times

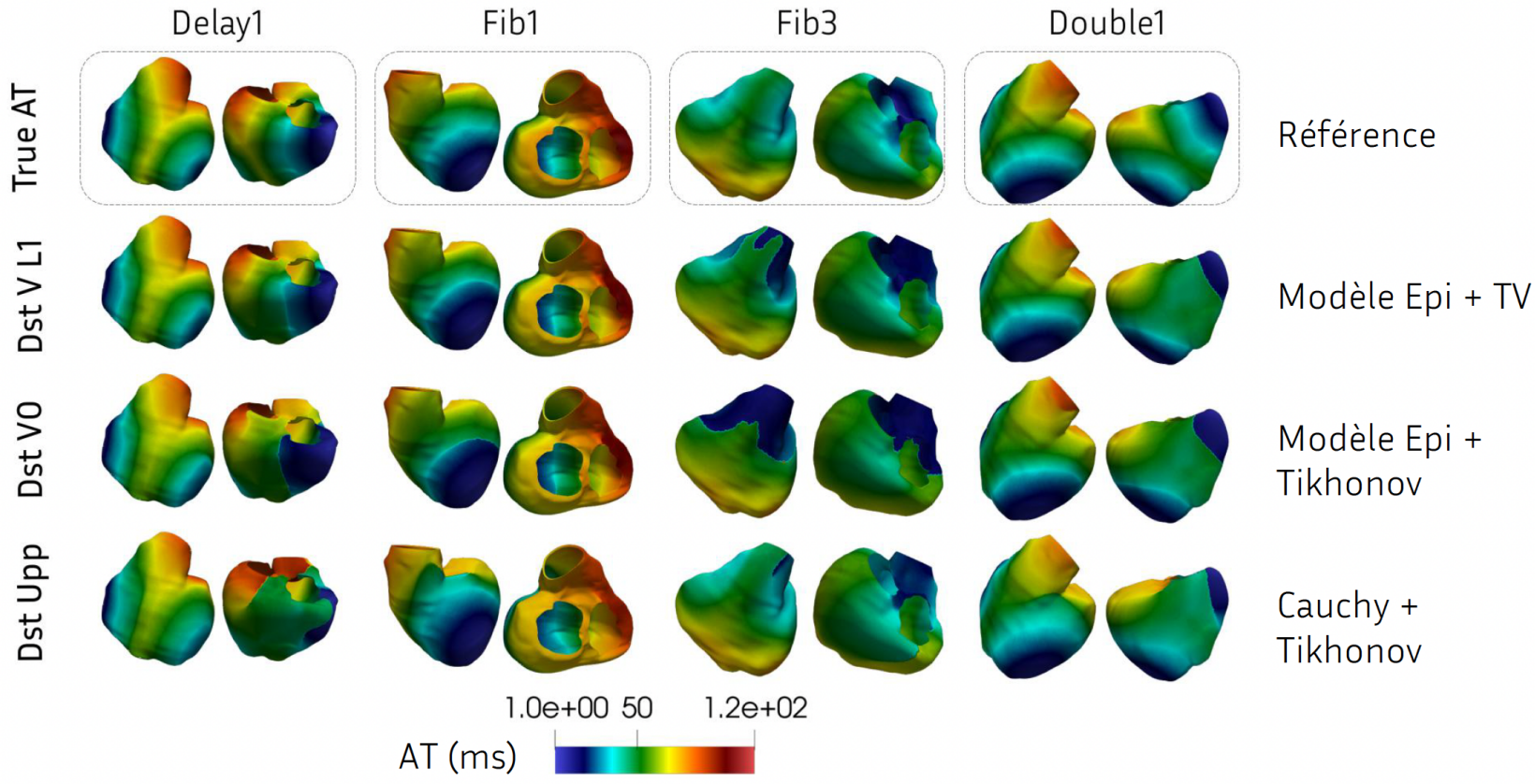

Partial conclusion

- New epicardial model, applicable for ECGi
- Possibility to add informations about conductivities, scars... in the cardiac tissue
- Possibility to take into account the specific behaviour of v (action potential)
- Validation on experimental ex-vivo data coming soon

Electrical impedance tomography (EIT)

Joint work : Jérémi Dardé, Niami Nasr

- Non-invasive reconstruction of conductivities from electrical measurements on the domain boundary
- Active electrodes set-up : complementary to ECGi
- Used in clinical routine for pulmonary ventilation monitoring, breast cancer detectiion, ..., not yet in electrocardiography

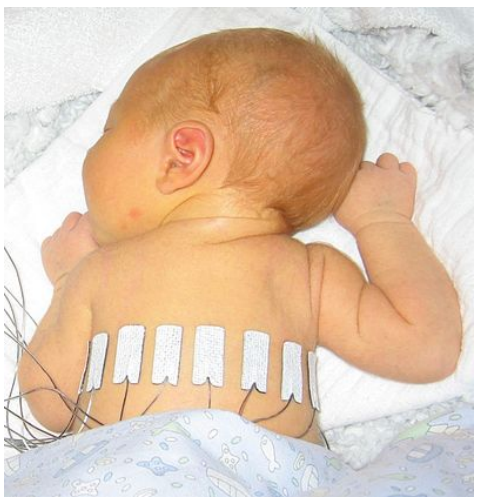

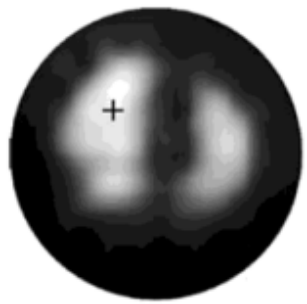

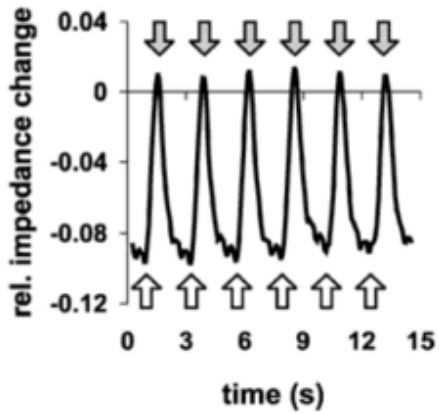

(Wikipedia, from S. Heinrich et al., Intensive Care Med., 2006)

Electrical impedance tomography (EIT)

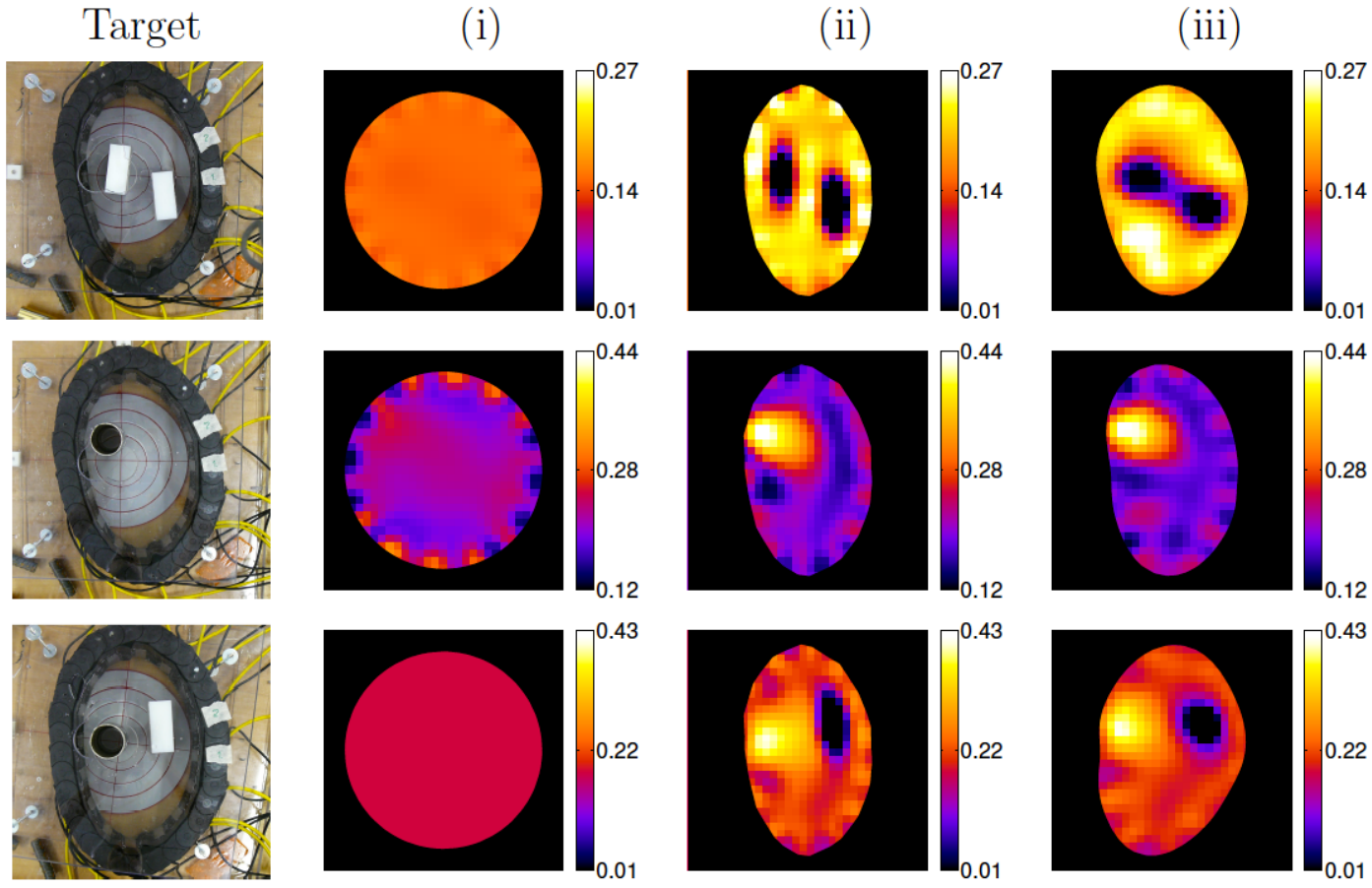

Dardé et al, SIAM J. Imaging Sci. 2013

Electrical impedance tomography (EIT)

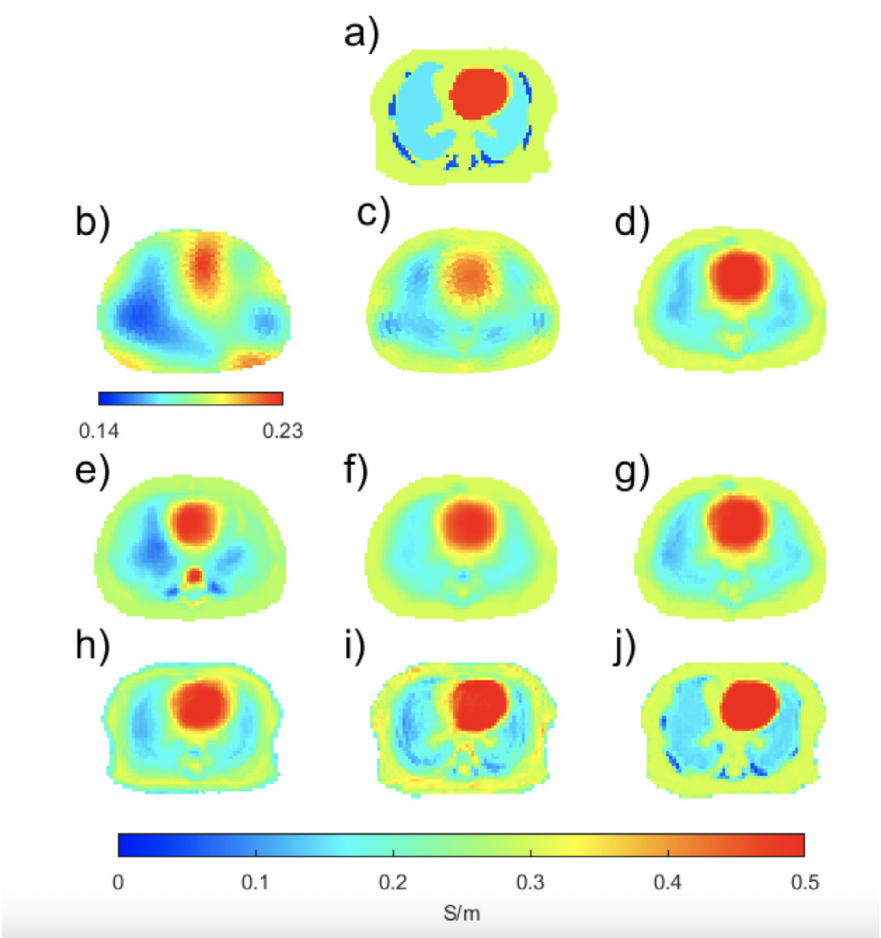

Fig. 8. A selected subject with a normal heart. Each subfigure shows a different reconstruction method based on the simulated data. All images are displayed in DICOM orientation. The NOSER method is on its own color scale. (a) Ground truth conductivity. (b) NOSER reconstruction. (c) Mean baby initial guess method. (d) Mean baby initial guess with Schur complement. (e) Eigenbaby method. (f) Eigenbaby with Schur complement. (g) Schur complement method. (h) Schur complement with boundary estimation. (i) End-to-end machine learning method. (j) Post-processing machine learning method.

EIT : direct problem modelling

"Complete electrode model" : takes into account the effect of metallic electrodes, contact impedance z_m on electrode m

Find $u \in H^1(\Omega)$ and $U \in \mathbb{R}^M_\diamond$ such that

$$\begin{cases} \nabla \cdot (\sigma \nabla u) &= 0 \text{ in } \Omega \\ u + z_m \sigma \partial_\nu u &= U_m \text{ on } E_m, \\ \sigma \partial_\nu u &= 0 \text{ on } \partial\Omega \setminus \overline{E}, \\ \displaystyle\int_{E_m} \sigma \partial_\nu u \, ds &= I_m. \end{cases}$$

with E_m electrode m, z_m associated impedance, $I \in \mathbb{R}^M_\diamond$ current and

$$\mathbb{R}^M_\diamond = \left\{ I \in \mathbb{R}^M, \sum_{k=1}^{M} I_k = 0 \right\},$$

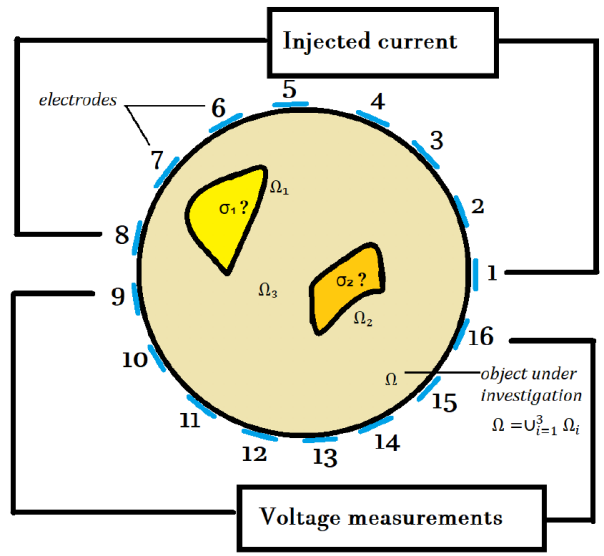

Image from A. Velasco PhD thesis

EIT : direct problem modelling

"Smoothened electrode model" : regularized model + penalization

Find $u \in H^1(\Omega)$ and $U \in \mathbb{R}^M_\diamond$ such that

$$\begin{cases} \nabla \cdot (\sigma \nabla u) &= 0 \text{ in } \Omega \\ \sigma \partial_\nu u &= \xi(U_m - u) \text{ on} \\ \sigma \partial_\nu u &= 0 \text{ on } \partial\Omega \setminus \overline{E}, \\ \displaystyle\int_{E_m} \sigma \partial_\nu u \, ds + \epsilon \delta^1_m U_m &= I_m . \end{cases}$$

ξ function ≥ 0 on $\partial\Omega$ satisfying

- $\xi \equiv 0$ on $\partial\Omega \setminus \overline{E}$
- $\xi \neq 0$ on each E_m

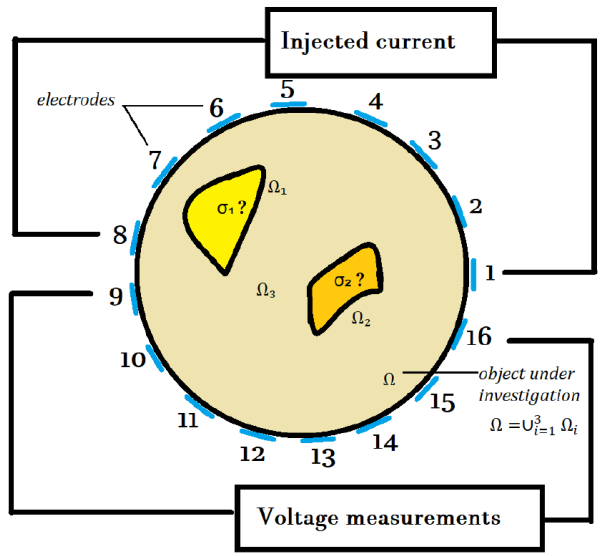

Image from A. Velasco PhD thesis

$u(\sigma, I)$, $U(\sigma, I)$ = solution for given σ and I

Discretization in complex geometries

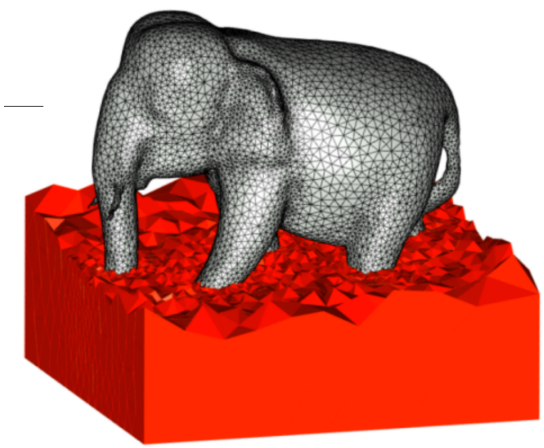

Sources : Mmg3d site et Wami Delthorn, a legos addict on Flickr

- Mesh adapted to geometry :
  - difficult to create, to adapt if moving geometry
  - natural adaptive refinement
  - easy to discretize equations on it
- Cartesian mesh :
  - no work with the mesh (nor complex partioning for parallel computing)
  - convenient for medical images (voxels)
  - loss of accuracy due to uniform refinement,
  - two different states with different properties can exist in one single cell : usual schemes not appropriate anymore

$\Rightarrow$ Development of "Immersed boundary methods"

Discretization strategy

Development of "Immersed boundary methods"
Compromise between accuracy and algorithmic complexity :

- Finite-difference schemes : easy to implement (and parallelize)
- Use sub-cell resolution taking into account the interface location

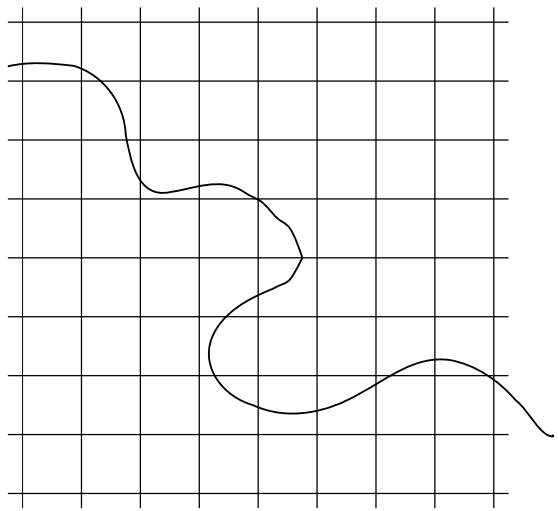

Discretization strategy

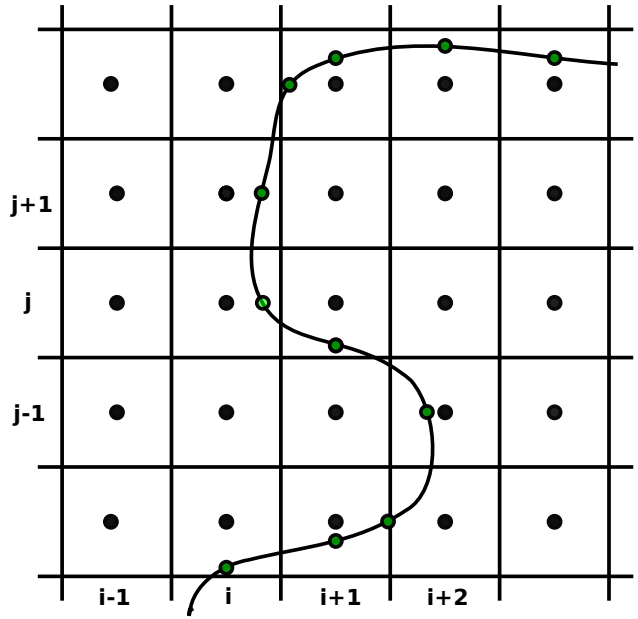

- Creation of additionnal unknowns on the interface
  - used to discretize the elliptic operator on each side of the interface
  - obtained by a discretization of jump conditions across the interface
- Cons : additional unknowns...
- Pros : additional unknowns !

Which accuracy near interface ?

To obtain a first-order convergence (L^∞ norm), we need an approximation (truncation) error

- zeroth order for elliptical operator near the interface $\nabla \cdot (\sigma \nabla u)$
- first-order for fluxes at the interface $\sigma \partial_\nu u$
- first-order for integral formula on each electrode $\int_{E_m} \sigma \partial_\nu u$

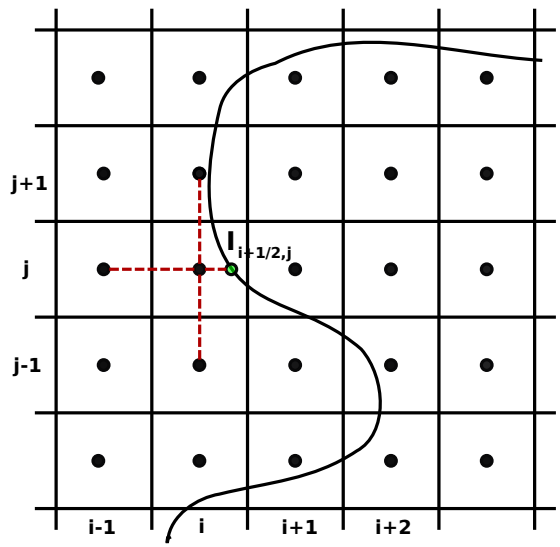

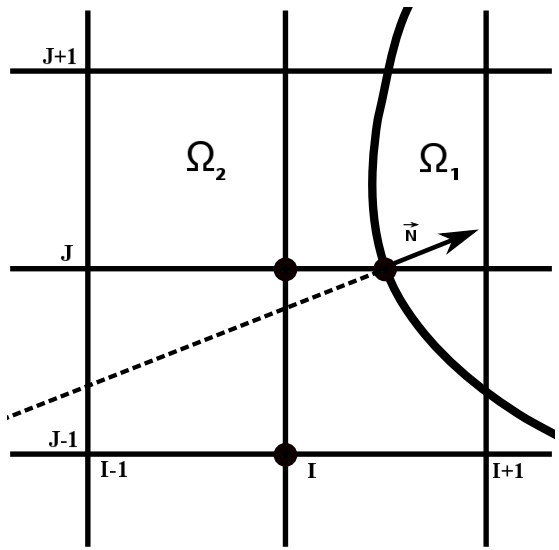

Which accuracy near interface ?

Quadrature formula on the electrodes :

- Discrete Dirac function (Smereka, JCP, 2000)
- built as the source term for a discrete Green function discretized with an immersed boundary method

$$
\begin{aligned}
-\Delta G &= 0 \text{ in } \Omega, \\
[\partial_n G] &= 1 \text{ on } \Gamma, \\
[G] &= 0 \text{ on } \Gamma.
\end{aligned}
$$

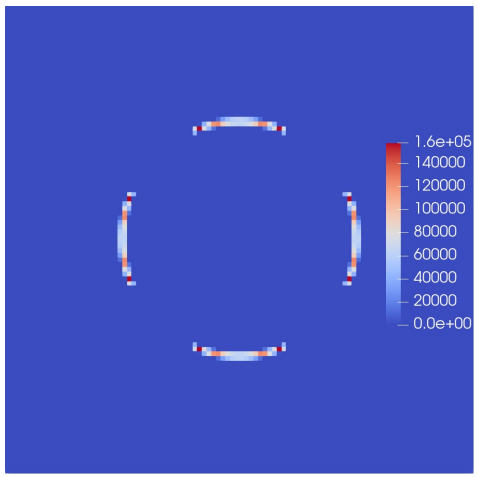

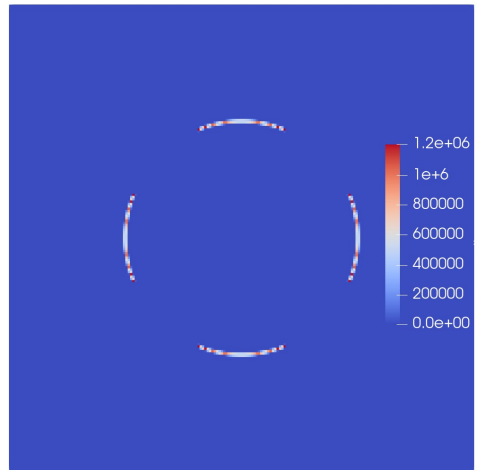

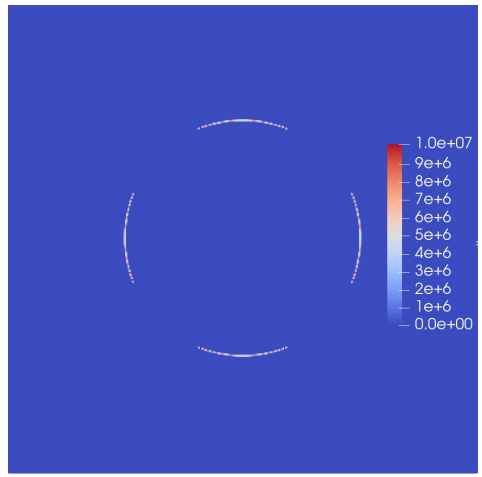

Discrete Dirac functions on electrodes, N = 100, 200, 400

Numerical convergence : solution and its gradient

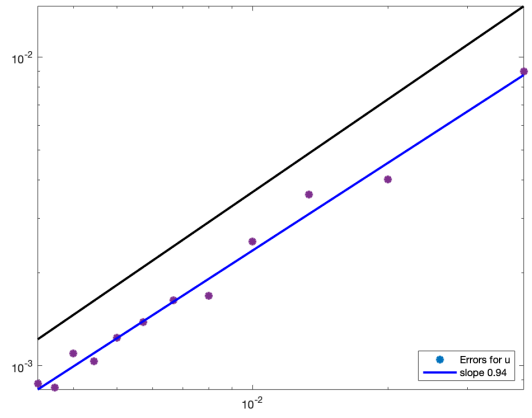

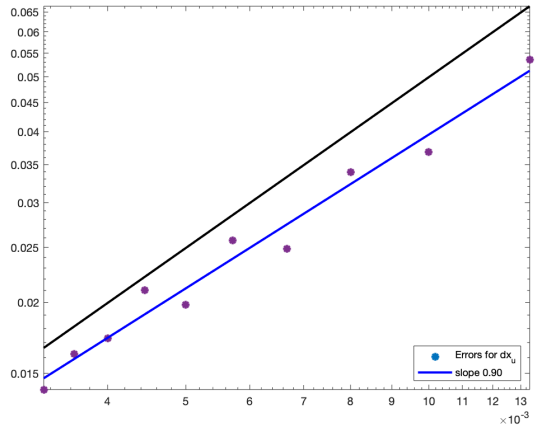

Reference solution : $u(x, y) = e^{(x^2+y^2)}$

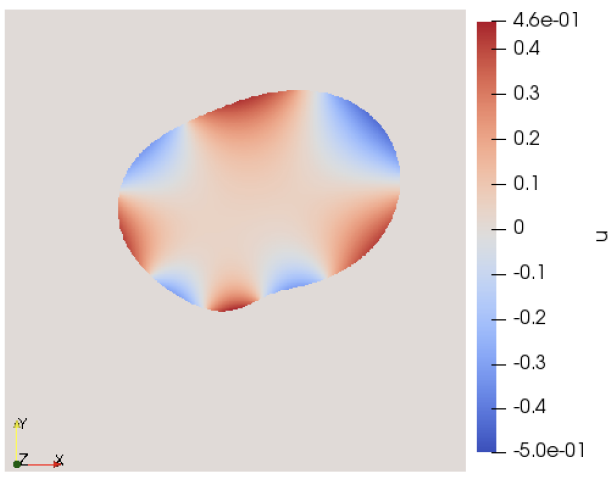

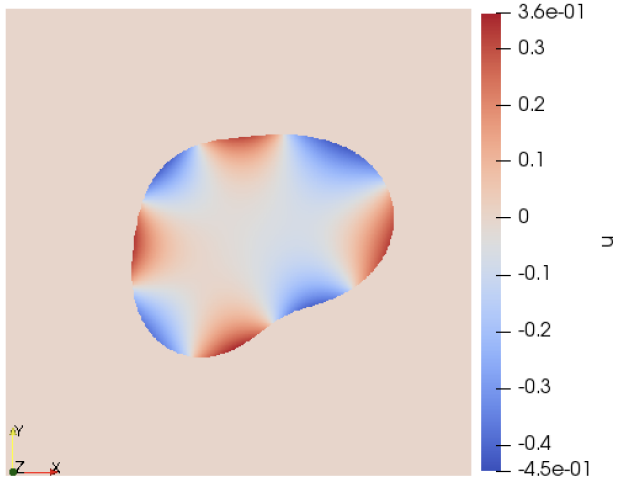

Theoretical study of the convergence

- A_h matrix of linear system arising from discretization U_h solution, f_h source term

$$A_h U_h = f_h$$

- Approximation (truncation) error :

$$\tau(P) = \begin{cases} O(h^2) \text{ for elliptic operator on regular nodes}, \\ O(1) \text{ for elliptic operator on irregular nodes}, \\ O(h) \text{ for flux conditions on interface points}, \\ O(h) \text{ for integrals on electrodes} \end{cases}$$

- The local error $e_h = U_h - U_{exact}$ satisfies the linear system :

$$A_h \, e_h = \tau_h$$

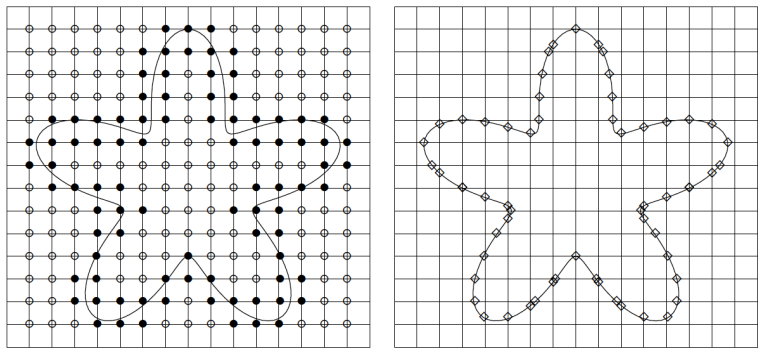

Ω_h : regular grid nodes $\circ$, Ω_h^* : irregular nodes $\bullet$,
Σ_h : interface points $\diamond$, E_h = electrode values

Strategies : FEM vs FV vs FD

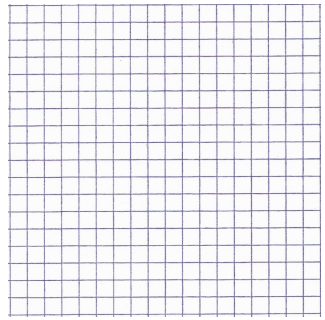

On a cartesian grid the same discretization matrix can be obtained with the 3 classes of methods, but different strategies for convergence :

- FEM : coercivity + Cea lemma + interpolation thm $\Rightarrow$ H^1-norm cv
- FV : coercivity + consistency + Poincaré inequality $\Rightarrow$ H^1-norm cv
- FD : monotonicity + discrete maximum principle $\Rightarrow$ L^∞-norm cv

Most convergence studies for FD methods with complex boundaries obtained with FEM techniques

- But loss of the "explicit character" of FD methods !
- L^∞-norm provides informations about accuracy near interfaces

Strategy

- The local error satisfies the linear system : $A_h e_h(P) = \tau(P) \quad \forall P \in \Omega_h$
- Naive estimate : $||e_h||_\infty \leq ||A_h^{-1}||_\infty ||\tau_h||_\infty$
- Not enough accurate here because $||\tau_h||_\infty = O(1)$
- Look for estimates by blocks of A_h^{-1}

$$e_h = \underbrace{\begin{pmatrix} \overbrace{\cdots\cdots\cdots}^{\sum a_{i,j}^{-1}=O(1)} & \overbrace{\cdots}^{\sum a_{i,j}^{-1}=O(h)} & \overbrace{\cdots}^{\sum a_{i,j}^{-1}=O(1)} \\ \cdots\cdots\cdots & \cdots & \cdots \\ \cdots\cdots\cdots & \cdots & \cdots \\ \cdots\cdots\cdots & \cdots & \cdots \\ \cdots\cdots\cdots & \cdots & \cdots \\ \cdots\cdots\cdots & \cdots & \cdots \end{pmatrix}}_{A_h^{-1}} \cdot \overbrace{\begin{pmatrix} O(h^2) \\ \vdots \\ O(h^2) \\ \hline O(1) \\ \vdots \\ O(1) \\ \hline O(h) \\ \vdots \\ O(h) \end{pmatrix}}^{\tau} = O(h)$$

Discrete Green functions

- For each point Q of the discretization, define the discrete Green's function $G_h(:,Q) = \Big(G_h(P,Q)\Big)_{P\in\Omega_h\cup\Sigma_h}$ as the solution of :

$$\left\{ \begin{array}{c} A_h G_h(:,Q)(P) = \left\{ \begin{array}{ll} 0, & P \neq Q \\ 1, & P = Q \end{array} \right. \qquad P \in \Omega_h \cup \Sigma_h, \\ G_h(P,Q) = 0, \text{on boundary.} \end{array} \right.$$

- Each $G_h(:,Q)$ is a column of A_h^{-1}

$$u_h(P) = \sum_Q G_h(P,Q)\,(A_h u_h)(Q)$$

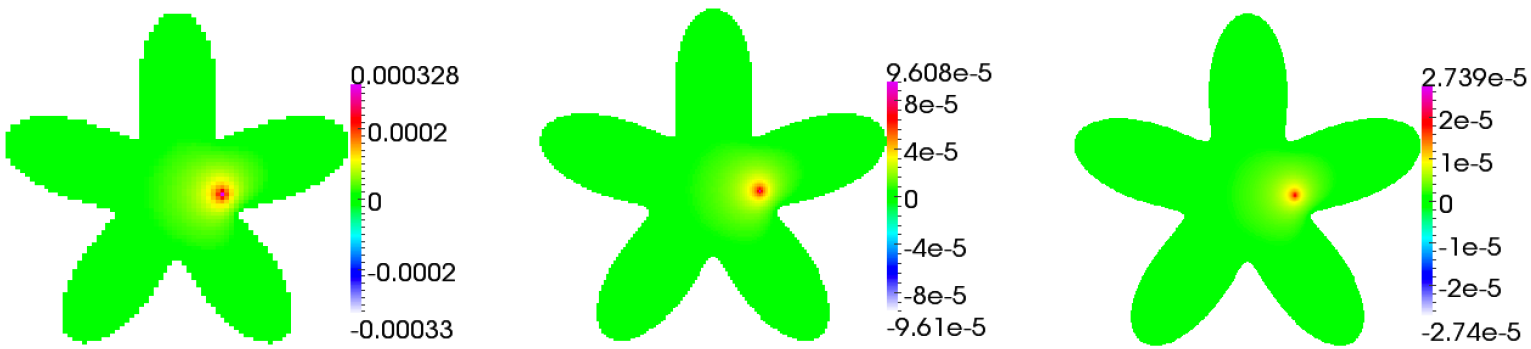

Discrete Green functions, 100^2, 200^2 and 400^2 grid points

Application of a discrete maximum principle

Theorem

(Ciarlet, 70) Let S be a subset of grid nodes, $\alpha > 0$ and W a discrete function s.t. :

$$\begin{cases} W(P) \equiv 0 \quad \forall P \in \Gamma_h, \\ (A_h W)(P) \geq 0 \quad \forall P \in \Omega_h, \\ (A_h W)(P) \geq \alpha^{-i} \text{ for all } P \in S. \end{cases}$$

If A_h is monotone then

$$\sum_{Q \in S} G_h(P, Q) \leq \alpha^i W(P).$$

Theoretical study of the convergence

- Prove that the matrix is monotone :

  requires to prove that if the minimum of U_h is on an interface point then the discrete flux on this point is negative

- Use discrete maximum principle and ad hoc functions to obtain estimates

$$\sum_{Q \in \Omega_h \cup \Sigma_h \cup E_h} G_h(P,Q) \leq O(1)$$

$$\sum_{Q \in \Omega_h^*} G_h(P,Q) \leq O(h)$$

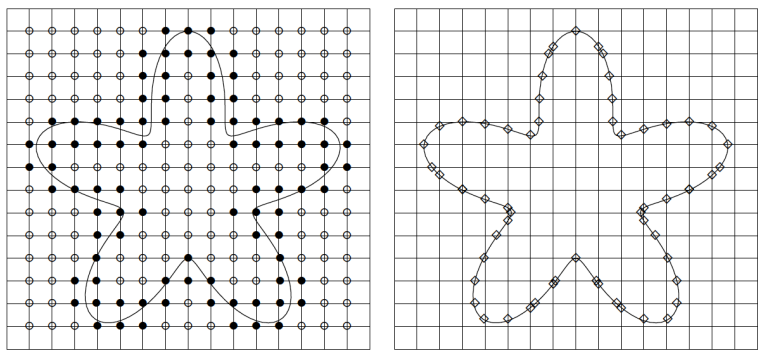

Ω_h : regular grid nodes $\circ$, Ω_h^* : irregular nodes $\bullet$,
Σ_h : interface points $\diamond$, E_h = electrode values

Convergence analysis

$$\sum_{Q \in \Omega_h \cup \Sigma_h \cup E_h} G_h(P,Q) \leq O(1)$$

$$\sum_{Q \in \Omega_h^*} G_h(P,Q) \leq O(h)$$

$$e_h = \underbrace{\begin{pmatrix} \overbrace{\cdots\cdots\cdots}^{\sum a_{i,j}^{-1} = O(1)} & \overbrace{\cdots}^{\sum a_{i,j}^{-1} = O(h)} & \overbrace{\cdots}^{\sum a_{i,j}^{-1} = O(1)} \\ \cdots\cdots\cdots & \cdots & \cdots \\ \cdots\cdots\cdots & \cdots & \cdots \\ \cdots\cdots\cdots & \cdots & \cdots \\ \cdots\cdots\cdots & \cdots & \cdots \\ \cdots\cdots\cdots & \cdots & \cdots \\ \cdots\cdots\cdots & \cdots & \cdots \end{pmatrix}}_{A_h^{-1}} \cdot \overbrace{\begin{pmatrix} O(h^2) \\ \vdots \\ O(h^2) \\ \hline O(1) \\ \vdots \\ O(1) \\ \hline O(h) \\ \vdots \\ O(h) \end{pmatrix}}^{\tau} = O(h)$$

Negative terms in discrete elliptic operator

$$F(x,y) = \log(\frac{C}{r}) \text{ with } r = \sqrt{x^2 + y^2 + h^2}.$$

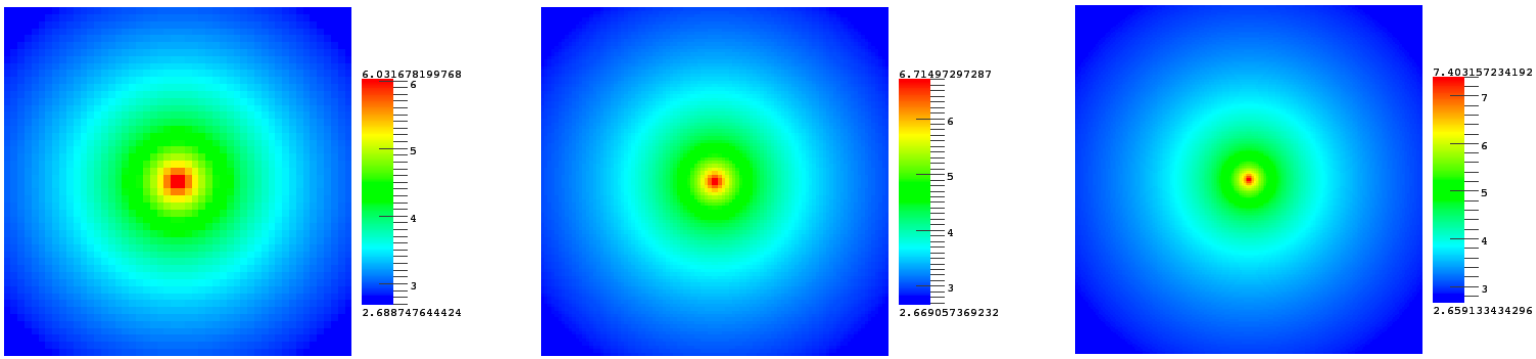

Discrete version of F, $N = 50, 100, 200$

Negative terms in discrete elliptic operator

$$F(x,y) = \log(\frac{C}{r}) \text{ with } r = \sqrt{x^2 + y^2 + h^2}.$$

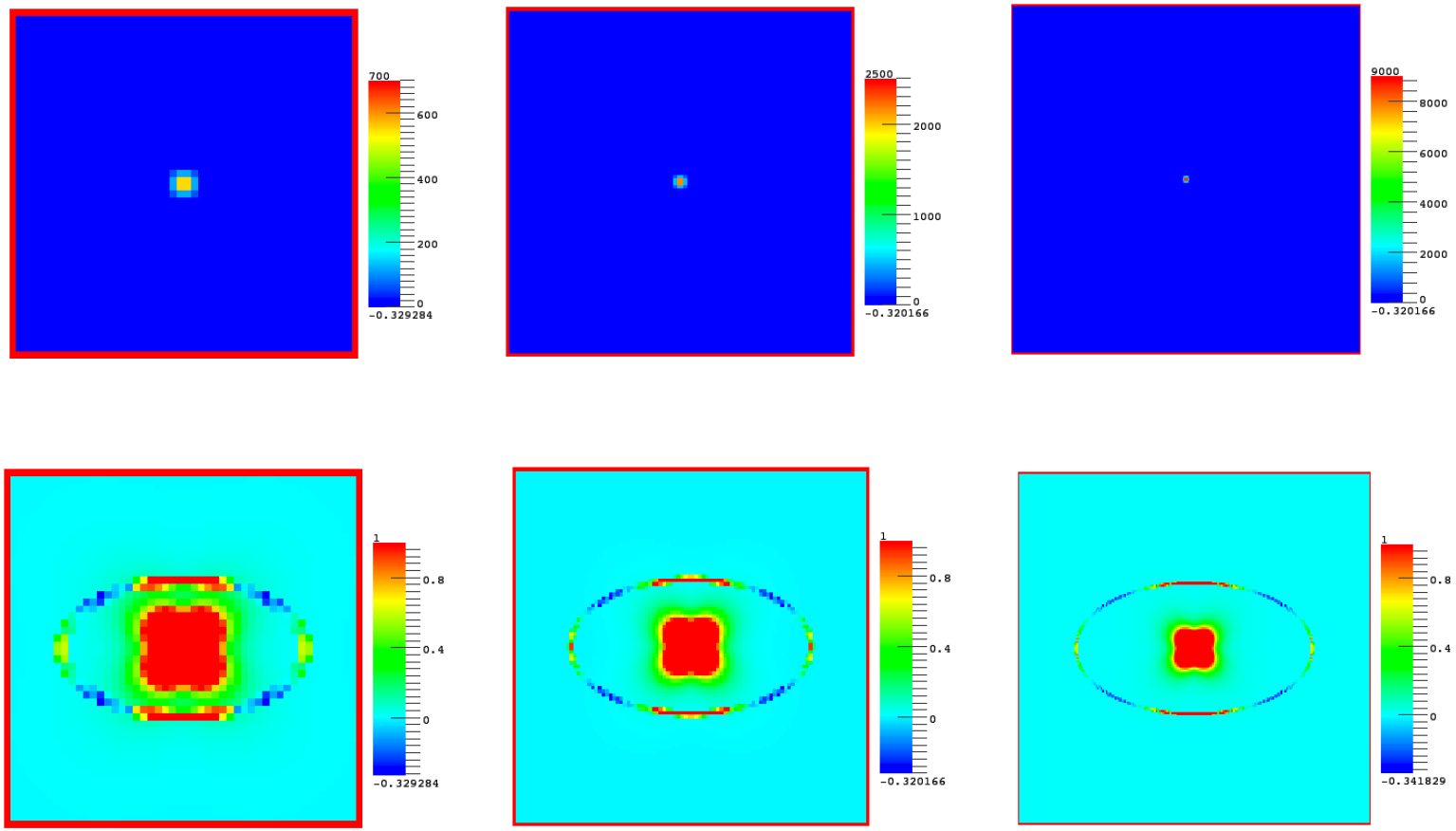

Discrete operator applied to F, $N = 50, 100, 200$

Variant of discrete maximum principle

Let S and $\tilde{S}$ be two subsets of points, W a discrete function with $W \equiv 0$ on $\delta\Omega_h$, and $\alpha > 0$, $\beta > 0$ such that :

$$\begin{cases} (A_h W)(P) \geq 0, \quad \forall P \in \Omega_h \cup \Sigma_h \setminus \tilde{S}, \\ (A_h W)(P) \geq \alpha^{-i}, \quad \forall P \in S, \\ (A_h W)(P) \geq -(\beta^{-j}), \quad \forall P \in \tilde{S}. \end{cases}$$

Then

$$\sum_{Q \in S} G_h(P,Q) \leq \alpha^i W(P) + \alpha^i \beta^{-j} \sum_{Q \in \tilde{S}} G_h(P,Q)$$

What about the gradient ?

- Numerical convergence : observed with order 1
- In literature : a few results on interior regularity for rectangular grids
- For the while : first-order convergence on rectangular domain

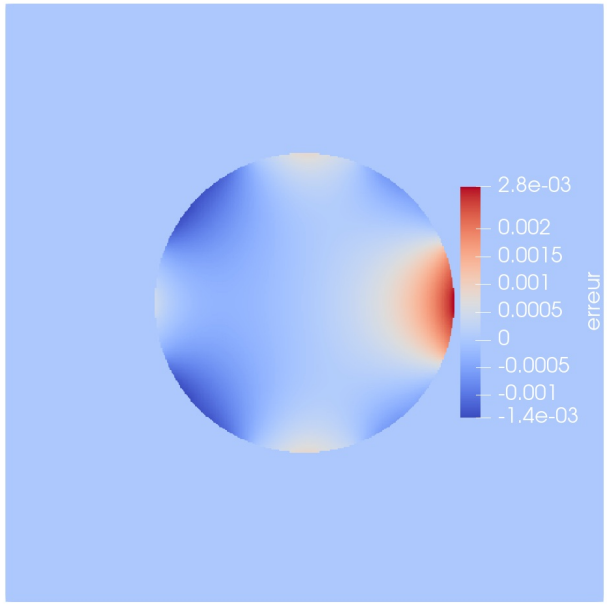

Numerical error computed for a smooth solution, N = 400

EIT : direct problem modelling

"Smoothened electrode model" : regularized model + penalization

Find $u \in H^1(\Omega)$ and $U \in \mathbb{R}^M_\diamond$ such that

$$\begin{cases} \nabla \cdot (\sigma \nabla u) &= 0 \text{ in } \Omega \\ \sigma \partial_\nu u &= \xi(U_m - u) \text{ on} \\ \sigma \partial_\nu u &= 0 \text{ on } \partial\Omega \setminus \overline{E}, \\ \displaystyle\int_{E_m} \sigma \partial_\nu u \, ds + \epsilon \delta^1_m U_m &= I_m . \end{cases}$$

ξ function ≥ 0 on $\partial\Omega$ satisfying

- $\xi \equiv 0$ on $\partial\Omega \setminus \overline{E}$
- $\xi \neq 0$ on each E_m

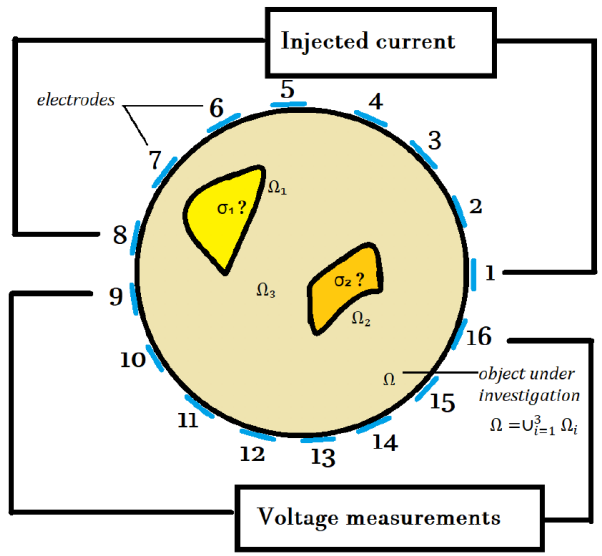

Image from A. Velasco PhD thesis

$u(\sigma, I)$, $U(\sigma, I)$ = solution for given σ and I

- For $I \in \mathbb{R}_\diamond^M$ fixé, $M : \sigma \mapsto \big(u(\sigma, I), U(\sigma, I)\big)$ is Fréchet-differentiable

$$M(\sigma + \delta\sigma) = M(\sigma) + (\delta u, \delta U) + o(\delta\sigma).$$

- For all σ et $\delta\sigma \in L^\infty(\Omega)$ tels que $\sigma > 0$ et $\sigma + \delta\sigma > 0$, $(\delta u, \delta U) \in H^1(\Omega) \times \mathbb{R}_\diamond^M$ is defined as the unique solution of

$$\begin{cases} \nabla \cdot (\sigma \nabla \delta u) &= -\nabla \cdot (\delta\sigma \nabla u(\sigma, I)) \text{ dans } \Omega \\ \sigma \partial_\nu(\delta u) &= \xi(\delta U_m - \delta u) - (\delta\sigma)\partial_\nu u(\sigma, I) \text{ sur } E_m, \\ \sigma \partial_\nu(\delta u) &= -(\delta\sigma)\partial_\nu u(\sigma, I) \text{ sur } \partial\Omega \setminus \overline{E}, \\ \int_{E_m} \sigma \partial_\nu(\delta u) &= -\int_{E_m} (\delta\sigma)\partial_\nu(u(\sigma, I)) \end{cases}$$

- Cost function to minimize :

$$F(\sigma) = \frac{1}{2}\|U(\sigma, I) - U_{mes}\|_{\mathbb{R}^M}^2 + \frac{\varepsilon}{2}\|\sigma - \sigma_*\|_{H^1(\Omega)}^2$$

- Cost function to minimize :

$$F(\sigma) = \frac{1}{2}\|U(\sigma, I) - U_{mes}\|^2_{\mathbb{R}^M} + \frac{\varepsilon}{2}\|\sigma - \sigma_*\|^2_{H^1(\Omega)}$$

- For $\delta\sigma \in H^1(\Omega)$, $\sigma + \delta\sigma > 0$, $t \geq 0$:

$$\begin{aligned} F(\sigma + t\,\delta\sigma) &\approx F(\sigma) + t(U(\sigma, I) - U_{meas}) \cdot \delta U + t\,\varepsilon(\delta\sigma, \sigma - \sigma_*)_{H^1(\Omega)} \\ &\approx F(\sigma) + t \int_\Omega \delta\sigma \underbrace{\Big(-\nabla u(\sigma, I) \cdot \nabla w + \varepsilon(\sigma - \sigma_*)\Big)}_{f} + \nabla(\delta\sigma) \cdot \underbrace{\varepsilon\nabla(\sigma - \sigma_*)}_{\mathbf{G}} \end{aligned}$$

with $(w, W) = (u, U)(U(\sigma, I) - U_{meas}, \sigma)$

- Let us define $\delta\sigma$ as the unique function in $H^1_0(\Omega)$ such that $\forall\, \tilde{\sigma} \in H^1_0(\Omega)$

$$\int_\Omega \nabla(\delta\sigma) \cdot \nabla\tilde{\sigma} + \delta\sigma\,\tilde{\sigma} = -\int_\Omega \mathbf{G} \cdot \nabla\tilde{\sigma} + f\,\tilde{\sigma}$$

Conductivities reconstruction

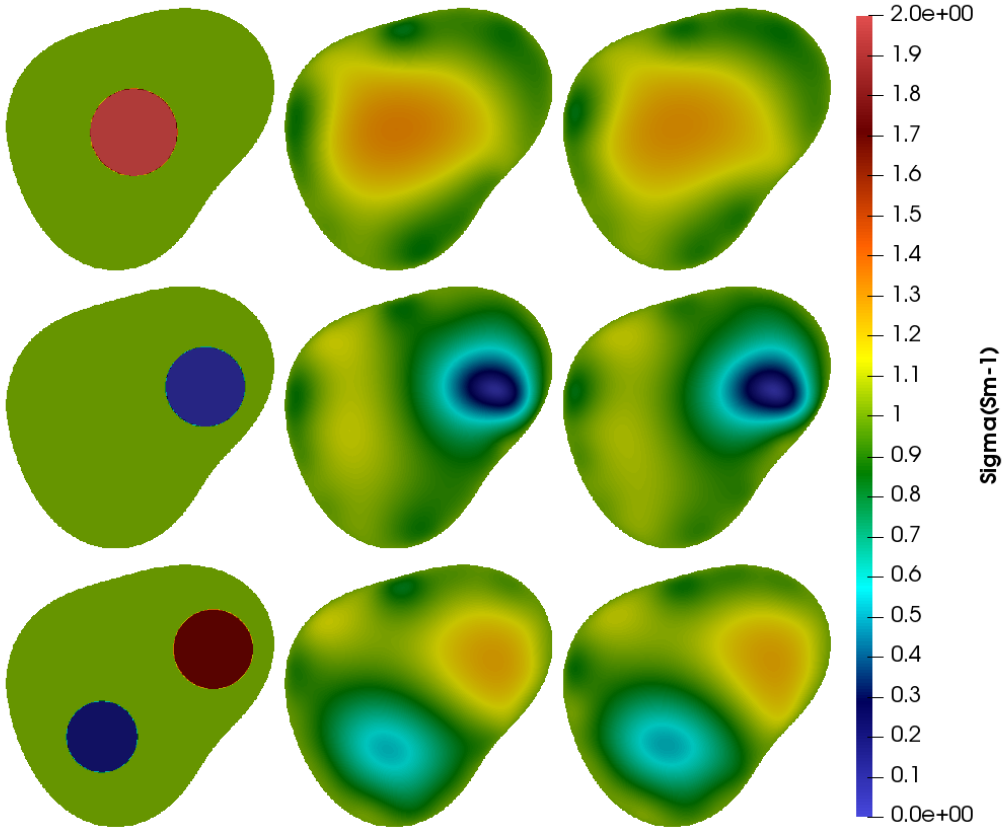

Left : reference, middle and right : reconstructions without and with noise, 16 electrodes

Reconstruction of shape and electrodes location

- Domain deformation :

$$F[h](x) = x + h(x), \quad x \in \partial\Omega, \quad h \in C^1(\partial\Omega, \mathbb{R}^n)$$

$$\partial\Omega_h = F[h](\partial\Omega) = \{y \in \mathbb{R}^n; y = F[h](x),\ x \in \partial\Omega\}$$

- Measurement operator :

$$\begin{aligned} R : B_d \times \mathbb{R}^M_\diamond &\longrightarrow \mathbb{R}^M \\ (\mathbf{h}, \mathbf{I}) &\longmapsto \mathbf{U}[\mathbf{h}] \end{aligned}$$

- Fréchet differentiability : there exists $R' : C^1(\partial\Omega, \mathbb{R}^n) \times \mathbb{R}^M_\diamond \longrightarrow \mathbb{R}^M/\mathbb{R}$ such that,

$$\lim_{\substack{h \to 0 \\ h \neq 0}} \frac{1}{\|h\|_{C^1}} \|R(h, I) - R(0, I) - R'h\|_{\mathbb{R}^M/\mathbb{R}} = 0, \quad \forall I \in \mathbb{R}^M_\diamond.$$

Reconstruction : sampling formula

Let $(\tilde{u}, \tilde{U}) \in H^{2-\epsilon}(\Omega)$, $\epsilon > 0$, be the solution for $\tilde{I} \in \mathbb{R}_{\diamond}^{M}$.
For all $(h, I) \in C^1(\partial\Omega, \mathbb{R}^n) \times \mathbb{R}_{\diamond}^{M}$

$$\sum_{m=1}^{M} (R'(h,I))_m \tilde{I}_m = -\sum_{m=1}^{M} \frac{1}{z_m} \int_{\partial E_m} (h.\nu_{\partial E_m})(U_m - u)(\tilde{U_m} - \tilde{u})\, ds$$

$$- \sum_{m=1}^{M} \frac{1}{z_m} \int_{E_m} h_\nu \Big((n-1)(U_m - u)H - \frac{\partial u}{\partial \nu} \Big) (\tilde{U_m} - \tilde{u})\, ds - \int_{\partial\Omega} h_\nu (\sigma \nabla u)_\tau . (\nabla \tilde{u})_\tau \, ds$$

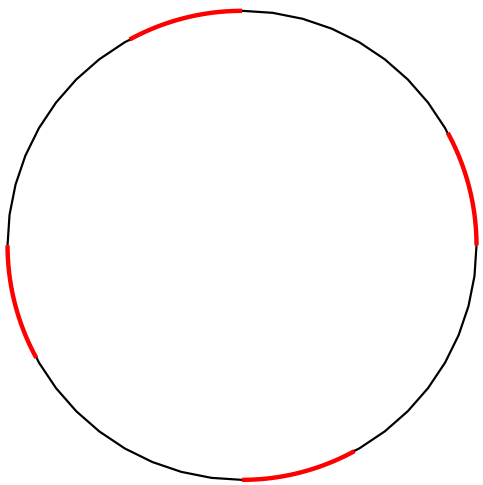

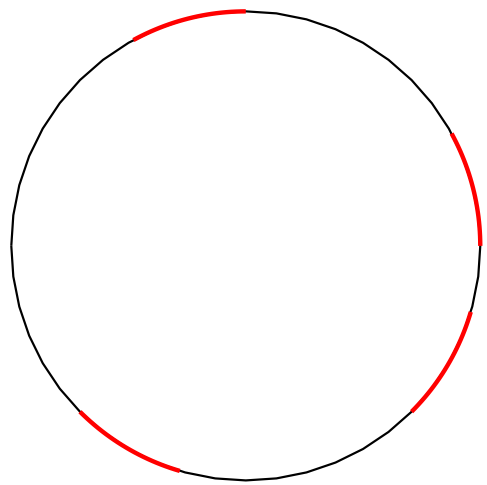

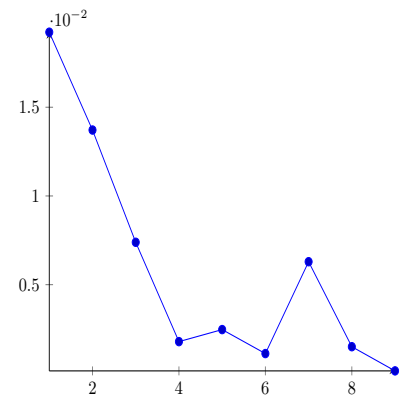

Left : reference configuration, middle : reconstruction, right : cost function

Reconstruction : sampling formula

Let $(\tilde{u}, \tilde{U}) \in H^{2-\epsilon}(\Omega)$, $\epsilon > 0$, be the solution for $\tilde{I} \in \mathbb{R}_{\diamond}^{M}$.
For all $(h, I) \in C^1(\partial\Omega, \mathbb{R}^n) \times \mathbb{R}_{\diamond}^{M}$

$$\sum_{m=1}^{M} (R'(h,I))_m \tilde{I}_m = -\sum_{m=1}^{M} \frac{1}{z_m} \int_{\partial E_m} (h.\nu_{\partial E_m})(U_m - u)(\tilde{U_m} - \tilde{u})\, ds$$

$$- \sum_{m=1}^{M} \frac{1}{z_m} \int_{E_m} h_\nu \Big((n-1)(U_m - u)H - \frac{\partial u}{\partial \nu} \Big) (\tilde{U_m} - \tilde{u})\, ds - \int_{\partial\Omega} h_\nu (\sigma \nabla u)_\tau . (\nabla \tilde{u})_\tau \, ds$$

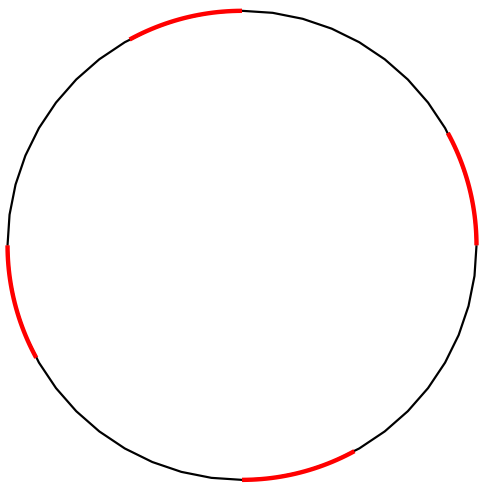

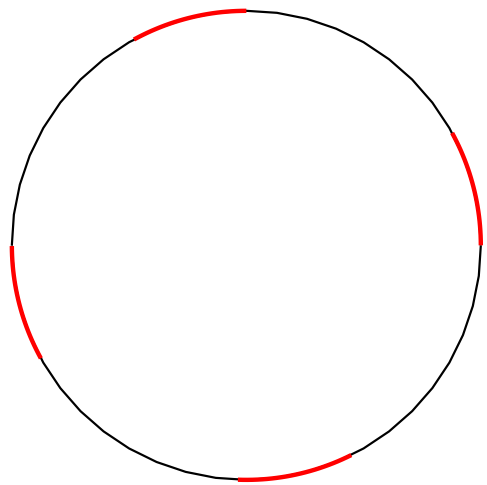

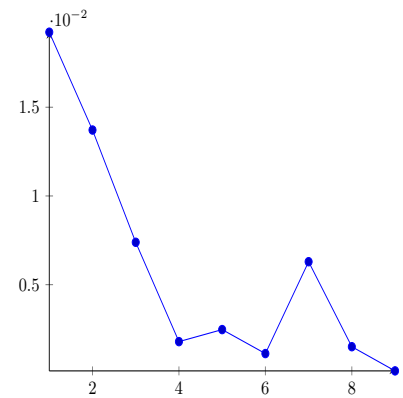

Left : reference configuration, middle : reconstruction, right : cost function

Geometries reconstruction

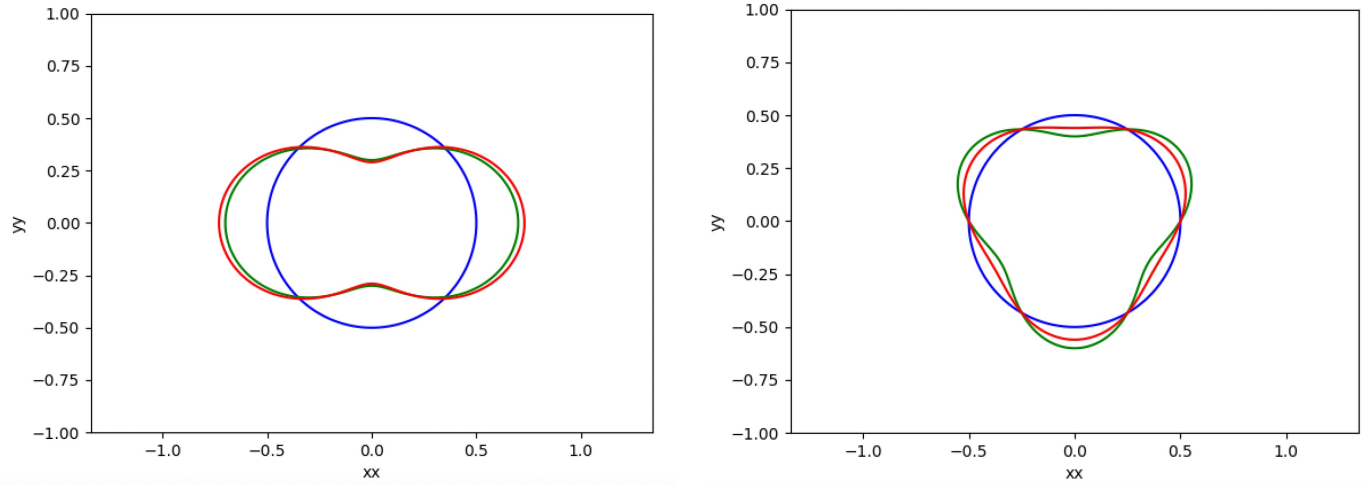

Blue : initialization, green : reference, red : reconstruction with 8 electrodes

Experimental perspectives at Liryc

Joint work : Suraj Baloda, Laura Bear (Signal processing team, Liryc)

- Torso tank : experimental set up for ex-vivo animal hearts
- Development of a coupled experimental ECGi-EIT set up

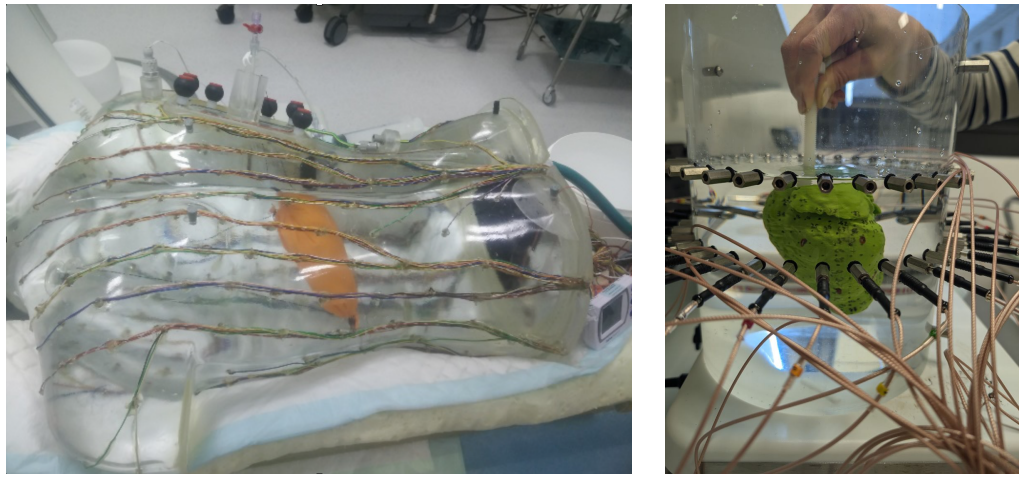

Torso tank set up, and set of active electrodes for EIT

RÉGION Nouvelle-Aquitaine

FONDATION GROUPE EDF

Experimental perspectives at Liryc

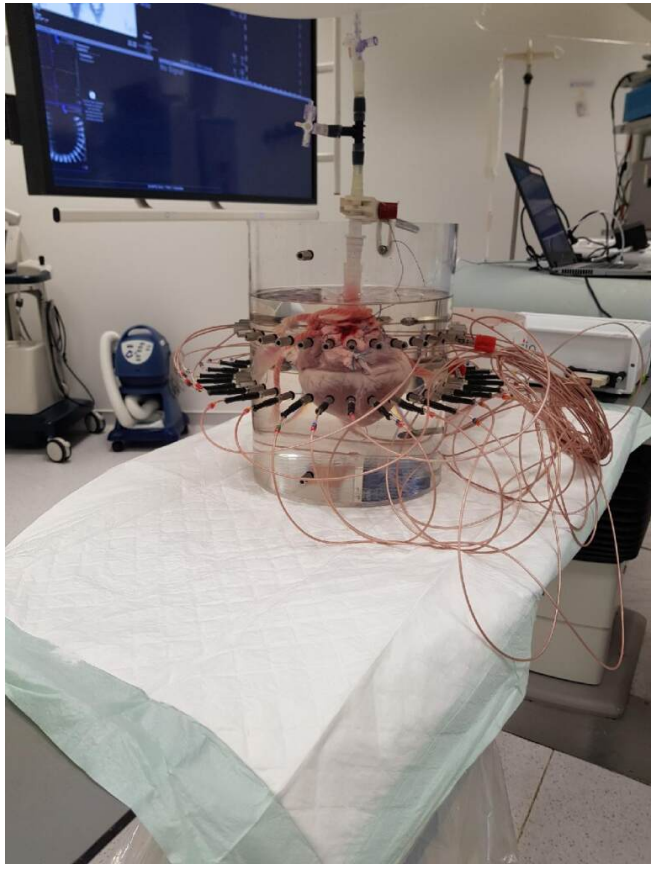

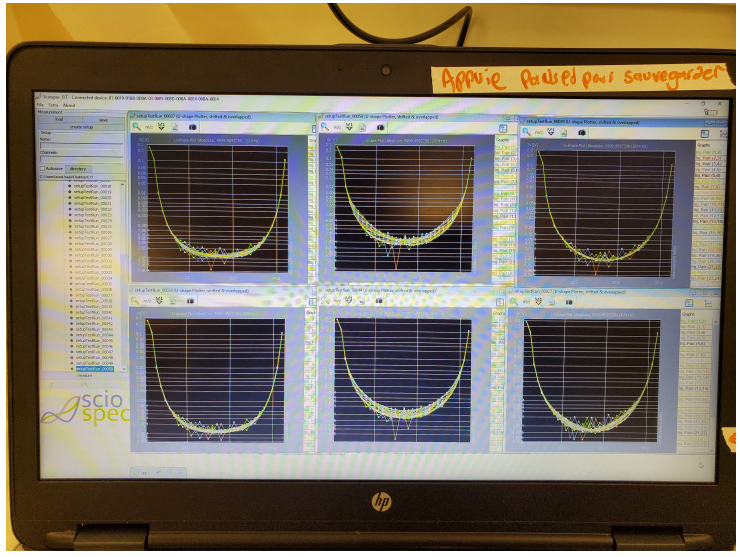

First tests with electrodes